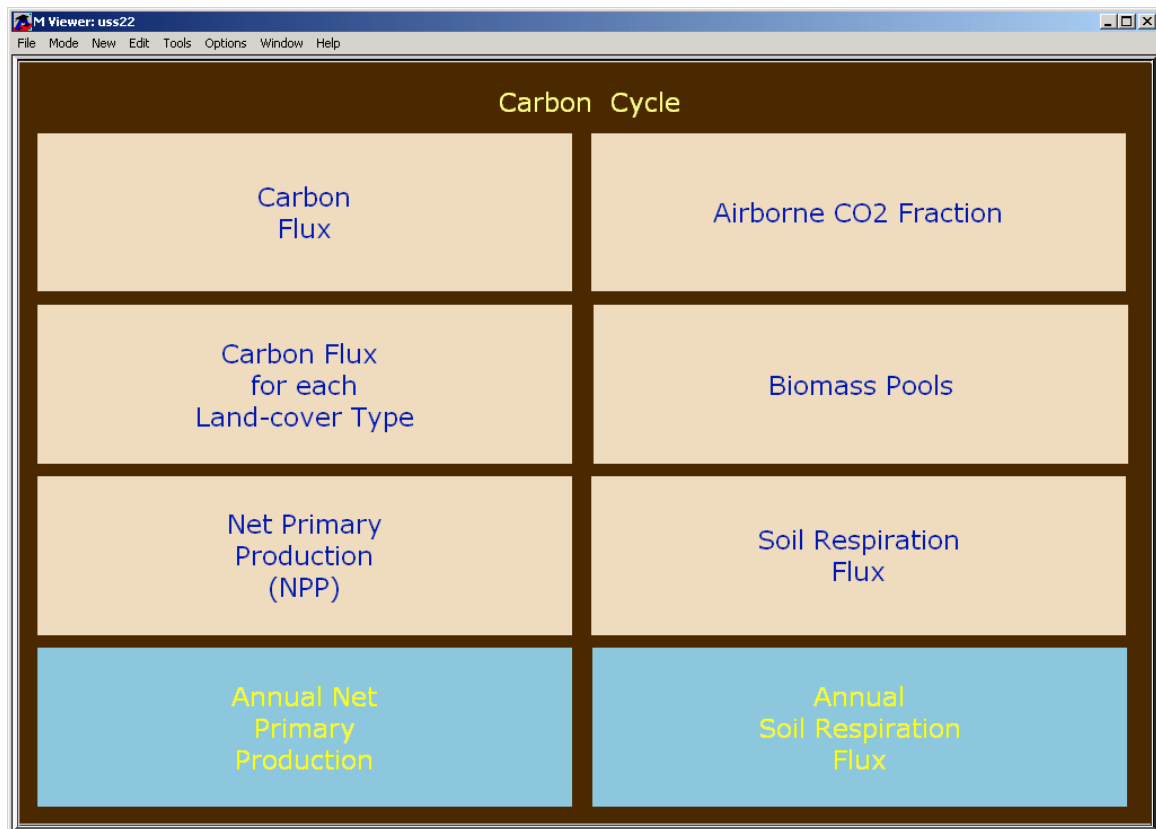


IMAGE 2.2

Carbon Cycle Analysis



August - September 2005

**Brinkman Climate Change
Consultant**

IMAGE 2.2 Carbon Cycle Analysis

Sander Brinkman*, Bart Strengers**, Jelle van Minnen**, Gert Jan***
Nabuurs, Eveline Trines****

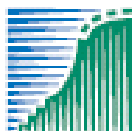
- * Brinkman Climate Change, Consultant
- ** MNP, Netherlands Environmental Assessment Agency
- *** Alterra, Wageningen University and Research Centre
- **** Treeness Consult



Contact:

Brinkman Climate Change
Plein 8c
2511CR The Hague, Netherlands
sander.brinkman@zonnet.nl

This analysis has been financed by the Dutch Ministry of Agriculture, Nature Management and Food Quality (LNV).



agriculture, nature
and food quality

Abstract

The IMAGE 2.2 model framework offers an integrated assessment of LULUCF and thus carbon sinks of both natural and managed systems and was therefore considered to be very useful in generating baselines for the IPCC WG III (Mitigation) chapters 8 (agriculture) and chapter 9 (forestry). However, according to some members of the writing team of chapters 8 and 9, the original IMAGE runs give a too large net carbon sink, which was not considered consistent with existing literature.

The sink is mainly found in the boreal and tropical regions (together 65% for SRES scenario B2 and 70% for SRES scenario A1f). For both regions, the natural CO₂ fertilisation effect is the major contributor to this carbon sink. Other factors, like changes in temperature and soil water availability (10 to 15%) and the time it takes to regrow to a more or less natural state (maximum 10%) appeared to be less contributing. Currently, a wide range of the natural CO₂ fertilisation effect on plant growth is debated in literature and IMAGE 2.2 is in the upper range. Therefore, new A1f and B2 runs were made with 50% lower natural CO₂ fertilisation and with no natural CO₂ fertilisation at all. The CO₂ fertilisation effect on agricultural crops was kept at the same high level, because farmers are supposed to adapt in such a way they can profit more from higher CO₂ levels from natural systems. The outcome of the new runs for the terrestrial net carbon balance is summarised in the table below.

There is an ongoing discussion in the IPCC WG III chapter teams 8 and 9 on the importance of CO₂ fertilisation in agriculture and forestry. According to the teams, the new runs cover the uncertainty range of and the discussion on CO₂ fertilisation, and are therefore used as baselines in the IPCC Fourth Assessment Report.

<i>Scenario / year (Pg C / yr)</i>	2000	2030	2050	2100
A1f original	0.32	3.26	4.97	7.33
A1f 50% fertilisation	-0.92	1.18	1.21	1.88
A1f No fertilisation	-1.14	-0.13	-0.41	-0.72
B2 original	0.45	2.35	3.58	4.01
B2 50% fertilisation	-0.71	-0.37	1.48	2.25
B2 No fertilisation	-0.96	-1.31	0.22	0.89

annual net carbon balance (uptake=positive, emissions=negative) for original IMAGE runs and for new baselines (sum of NEP and deforestation¹ (Pg C / yr))

Since this report shows that the CO₂ fertilisation effect of IMAGE is in the upper range, the CO₂ fertilisation factor will be updated in a next version.

Keywords: CO₂ fertilisation, carbon cycle, sink, IMAGE

¹ IMAGE deforestation fluxes include timber harvest fluxes

Table of Content

Abstract	4
1. Introduction	6
2. Methodology.....	9
3. Identifying the large net carbon sink.....	10
3.1 Regions and Land Cover Types.....	10
3.2 Areas.....	10
3.3 Carbon Fluxes.....	11
3.4 CO ₂ Fertilisation.....	12
3.5 Growth factor.....	13
3.6 Recovery period.....	14
4. Simulation experiments.....	15
4.1 Introduction	15
4.2 NPP: fertilisation versus climate growth factor.....	15
4.3 CO ₂ fertilisation.....	17
4.3.1 Global scale	17
4.3.2 Regional carbon dynamics.....	18
4.4 Grid cell analysis	19
4.5 Recovery period.....	20
5. New Baselines.....	23
5.1 Global scale	23
5.2 Regional carbon dynamics.....	24
6. Conclusions	26
Acknowledgement.....	27
Literature	28
Appendix A	29
Appendix B.....	30
Appendix C	32
Appendix D	34

1. Introduction

The Integrated Model to Assess the Global Environment (IMAGE-2.2) is an ecological-environmental framework that simulates the environmental consequences of human activities worldwide. It represents interactions between society, the biosphere and the climate system to assess issues like climate change, biodiversity and the structure of the energy system. The objective of IMAGE is to explore the long-term dynamics of global change as the result of interacting demographic, technological, economic, social, cultural and political factors.

The Intergovernmental Panel on Climate Change (IPCC) published a set of new scenarios in the Special Report on Emissions Scenarios (SRES) (IPCC, 2000) (see Appendix D). Contrary to the original SRES scenarios, the IMAGE scenarios do not focus solely on emissions, but also describe the possible environmental impacts of these scenarios. It should, however, be clear that the IMAGE scenarios represent only one of the many possible elaborations of the SRES scenarios. In this respect, they reflect the authors' interpretations and valuation of only a part of past and present events, behaviours and structures.

In the IMAGE 2.2 model, the terrestrial carbon cycle is modelled as integral part of the overall land-use, land-use change and forestry (LULUCF) system. The net flux of carbon between the atmosphere and the terrestrial system depends on the land cover, the atmospheric concentration of CO₂, and climate conditions. Land cover change is endogenous and is established at a 0.5x0.5 degree resolution. Land cover types distinguished include a range of natural biomes, from ice and desert to tropical forests, plus agricultural land and two classes of re-growth vegetation: on abandoned agricultural land and after clearing for timber production. The early versions of the model are described in detail by Klein Goldewijk et al. (1994) and Alcamo et al. (1998). The basic structure of the terrestrial carbon model in IMAGE version 2.2 has not changed in comparison with earlier versions of IMAGE (2.0 and 2.1). An important improvement is however that the calibration of the full carbon cycle starts in 1765. Historical anthropogenic CO₂ emissions (Marland et al., 2000) and the historical trend of oceanic C uptake (Joos et al., 1996) are used (1765-1970) to obtain a terrestrial uptake in the terrestrial carbon model that leads to a CO₂ concentration of 325 ppmv in 1970.

The terrestrial carbon model is driven by Net Primary Productivity (NPP, plant photosynthesis minus plant respiration), a function of climate, soil, atmospheric CO₂ concentration, altitude, land-cover type and land-cover history. NPP is allocated over the living biomass compartments, and then slowly shifts to the non-living biomass compartments, where it is decomposed and returns as CO₂ to the atmosphere. The allocation fractions and turnover times are defined for each land-cover type and C compartment.

Soil respiration is the C flux to the atmosphere resulting from the transformation of soil organic matter (litter, humus and charcoal). During decay of litter and dead roots, part is transformed into soil humus, while another (major) part is oxidized to CO₂ and lost to the atmosphere. An important part of the soil humus pool is also oxidized to CO₂ and lost to the atmosphere, while a small fraction is transformed into charcoal. Charcoal is a major carbon pool in many land-cover types. Its respiration flux is therefore significant, despite its long lifetime.

The terrestrial carbon cycle model calculates plant growth (=Net Primary Production or NPP) and allocates this to the living biomass pools (stems, branches, roots, leaves) based on fixed land cover type dependent allocation fractions. These pools have associated lifetime-values that determine how much carbon flows to the non-living carbon pools (litter, humus). Both the potential productivity of crops, including pasture, and the NPP of natural vegetation are influenced by climate change and water availability (together determining the length of the growing season) and the increasing atmospheric concentration of CO₂ leading to a CO₂ fertilisation effect.

The net C flux between the atmosphere and biosphere is called 'net ecosystem productivity' (NEP) and is equal to the NPP minus soil respiration. Negative values indicate a net release of CO₂, while positive values indicate a net uptake of CO₂ by the biosphere. NEP is influenced by land cover (changes) and soil and climatic factors.

The most important negative and positive feedback processes in IMAGE 2.2 on the build-up of CO₂ concentrations are CO₂ fertilisation and soil respiration respectively. The most important feedback is CO₂ fertilisation. Constant CO₂ fertilisation rapidly stabilises NPP. The impact of constant soil respiration is much less than that of CO₂ fertilisation. Although, soil respiration is the largest positive feedback, CO₂ fertilisation more strongly determines the final atmospheric CO₂ concentrations (Leemans et al, 2002).

Climate feedbacks (effect of temperature and CO₂ fertilisation on plant growth, and effect of climate on soil respiration) are calculated at monthly intervals by using different response functions dependent of temperature, soil water and species characteristics for each grid cell (Klein Goldewijk et al., 1995). These monthly values are aggregated to annual totals for use in C-balance calculations. However, the monthly resolution allows different plant responses in different seasons to be taken into account. This temporal resolution is also consistent with the downscaling of monthly climate-change patterns in the atmosphere-ocean system.

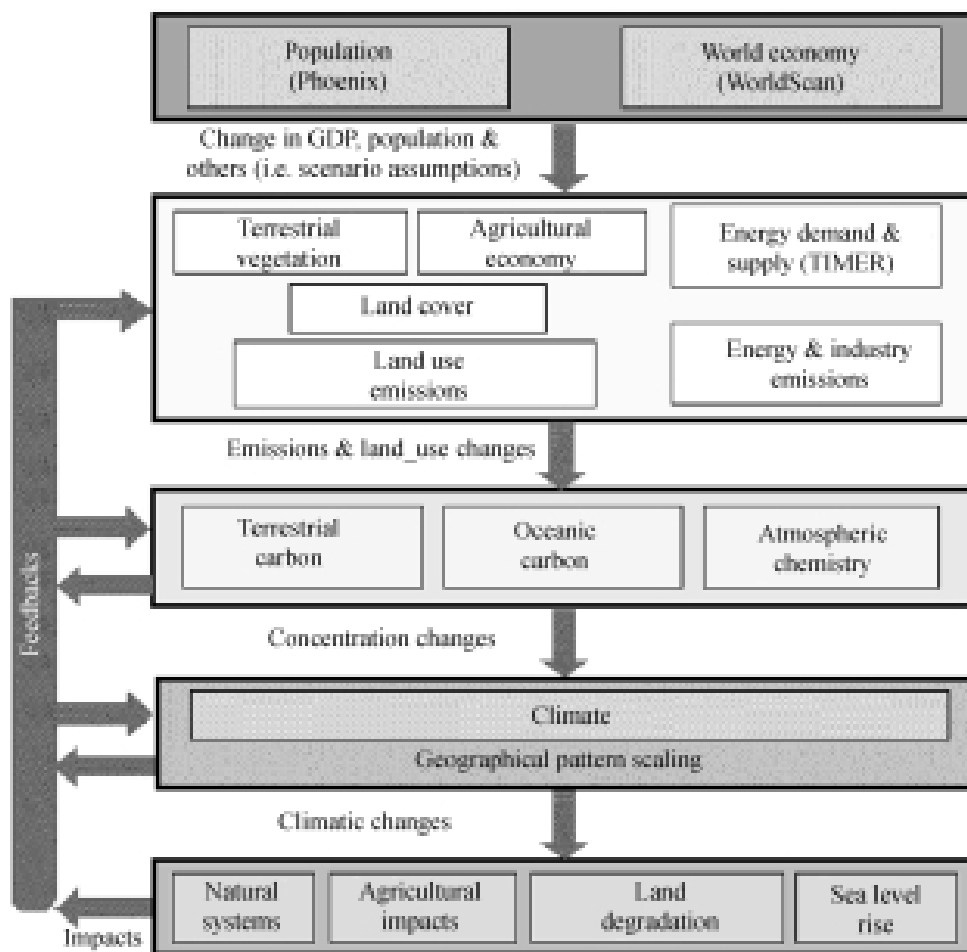


Fig. 1.1 The structure of IMAGE 2.2 (Leemans et al, 2002).

This analysis will concentrate on the A1f and B2 scenarios, since these are used by the IPCC Working Group III chapters 8 (agriculture) and 9 (forestry). The IPCC team of these chapters considered the current IMAGE carbon cycle results as not being ‘realistic’. One of the issues is the (too) large net carbon sink in the terrestrial module, as shown in the table below.

<i>Scenario / year</i> <i>(Pg C / yr)</i>	2000	2030	2050	2100
A1f	0.32	3.26	4.97	7.33
B2	0.45	2.35	3.58	4.01

*Annual net carbon sink in IMAGE 2.2
(sum of NEP and deforestation (Pg C / yr))*

Following the IPCC comments, an analysis has been carried out on the C-cycle balance in IMAGE 2.2. in order to identify what mechanisms and parameter settings in IMAGE could be responsible for these results and which could potentially be adjusted in the short term.

Alternative assumptions, suggested by the experts involved, have been tested in IMAGE to check their impact. Some potential causes for this (too) large net carbon sink might be found in the underlying land use scenarios (e.g. underestimated deforestation, overestimated productivity gains in agriculture, role of natural disturbances, etc.). Improvements in those parts of the model are already planned in various ongoing research activities, requiring more time, and are thus not pursued further in this analysis.

The carbon cycle will firstly be examined at the global level. Secondly, this will be done at the regional scale: as well per world region as per Land Cover Type (LCT). Thirdly, a grid cell analysis will be made to follow the carbon uptake (or release) for specific LCTs.

2. Methodology

Since the chapters 8 and 9 of Working Group III of the IPCC are mainly working with the scenarios A1f and B2, this analysis has been limited to these scenarios. Because the IMAGE team already made several extra runs for scenario A1b before, these were also used in this study.

The first step to take was to determine where the large sink has its origin: in which region(s) and for which land cover type(s) (LCT). IMAGE 2.2 identifies 18 regions and 18 land cover types, as shown below.

Land cover types	
Agricultural land	Temp. mixed forest
Extensive grassland	Temp. deciduous Forest
Regrowth forest (abandoned)	Warm / mixed forest
Regrowth forest (timber)	Grassland / steppe
Ice	Hot desert
Tundra	Scrubland
Wooded tundra	Savannah
Boreal forest	Tropical woodland
Cool conifer	Tropical forest

Regions	
Canada	Eastern Europe
USA	Former USSR
Central America	Middle East
South America	S-Asia
N-Africa	E-Asia
W-Africa	SE-Asia
E-Africa	Oceania
Southern Africa	Japan
OECD Europe	Greenland

When the most contributing regions and LCTs are identified, the next step was to find the cause for the large sink for that specific LCT. This is done by looking into:

- Changes in the size of LCTs
- full grown and regrowing vegetation fluxes
- soil fluxes and vegetation fluxes
- Net Primary Production (NPP), Soil Respiration Fluxes (SRF) and Net Ecosystem Production (NEP)

At some stages, the IPCC WG III chapter 8 and 9 authors have been asked to have a look at figures and data. They were invited to recommend recent literature on the relevant issues to corroborate parameter values and to give comments on the outcome of new model runs.

Finally, based on their comments and on presented literature some parameters were changed and new baseline runs were made. These runs have been recalibrated, in order to reproduce the past in terms of the atmospheric CO₂ concentration.

3. Identifying the large net carbon sink

3.1 Regions and Land Cover Types

First of all it was determined which land cover types and which regions are causing the sink. Given table 3.1, the land cover types responsible for the large sink are boreal forest, tropical woodland and tropical forest, for both scenarios A1f and B2.

The regions contributing most to the sink are: Former USSR (A1f and B2), South America (A1f and B2), Canada (A1f and B2), East Asia (A1f), Western Africa (A1f) and the USA (B2).

Table 3.1. Carbon fluxes (incl. full grown vegetation, regrowing vegetation and deforestation; positive=sink (NBP)) per year for three land cover types, six regions and the world total (Pg C / yr)

LCT & region	A1f				B2			
	2000	2030	2050	2100	2000	2030	2050	2100
Boreal forest	0.73	1.15	1.59	2.13	0.73	1.08	1.28	1.45
Tropical woodland	0.20	0.55	0.90	1.52	0.21	0.37	0.52	0.52
Tropical forest	0.43	0.80	1.05	1.49	0.43	0.66	0.75	0.79
Former USSR	0.46	0.79	1.19	1.58	0.42	1.00	1.25	1.31
South America	0.22	0.73	0.98	0.76	-0.03	0.70	0.67	0.37
Canada	0.22	0.38	0.53	0.60	0.18	0.39	0.49	0.53
East Asia	-0.08	0.07	0.14	0.25	-0.16	-0.12	0.31	0.28
Western Africa	0.17	0.14	0.37	0.40	0.13	-0.43	-0.12	0.31
USA	0.15	0.26	0.29	0.24	0.12	0.23	0.44	0.45
WORLD	0.40	3.21	4.75	7.33	0.54	1.72	3.67	4.23

3.2 Areas

The carbon fluxes in IMAGE 2.2 increase over time. Figure 3.1 shows that the areas of boreal forests in the former USSR and Canada are increasing (+13% and +10% resp.). However, the areas for tropical forests in South America and Western Africa are decreasing (21-28% and 25-63% resp.).

Therefore, we conclude in the tropical regions the area is of no influence for the large sink. For the boreal region the area might be a cause of the large sink.

As already said, this analysis project concentrates on the IMAGE C-cycle. Since the forest distribution is part of the land use module and not of the carbon cycle, it is not possible to change these within this project, if necessary at all. However, the carbon dynamics within the forests is obviously part of the carbon cycle model and covered in the following sections.

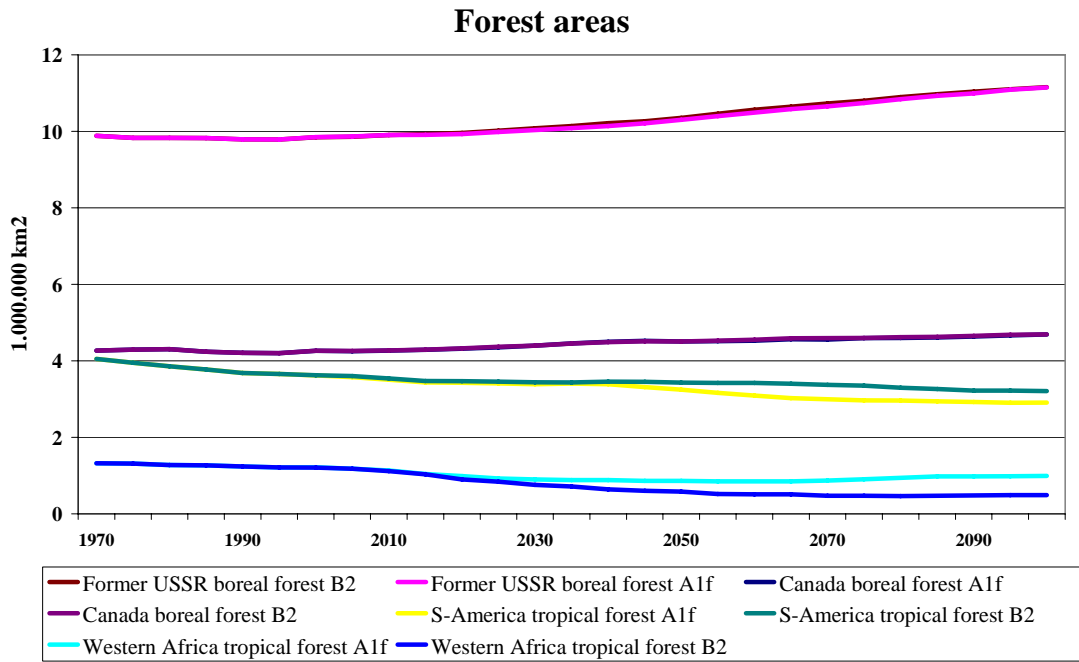


Figure 3.1 Forest areas over time for scenarios A1f and B2; Former USSR boreal forest, Canada boreal forest, South America tropical forest and Western Africa tropical forest.

3.3 Carbon Fluxes

The Net Ecosystem Production (NEP) is calculated by the Net Primary Production (NPP) minus the Soil Respiration Flux (SRF). The NPP is influenced by the CO₂ fertilisation effect (section 3.4) and climate change (section 3.5). The SRF exists of respiration from litter, humus and charcoal.

The first two figures in Appendix B show an increasing NPP for both A1f and B2, namely from 58 Pg C/yr in 1970 for both, to 91 and 81 Pg C/yr in the year 2100, respectively. The SRF increases from 57 to respectively 83 and 76 Pg C/yr. This means an NEP increase from 1 to 8 Pg C / yr for scenario A1f and from 1 to 5 Pg C/yr for scenario B2. Hence, either the SRF is too small, or the NPP is too large, or both.

The former USSR shows a largely increasing NPP for full grown boreal forests, which is steadily growing from 0.2 Pg C/yr in 1970 to 1.25 Pg C/yr in 2100 (Appendix A1). Full grown forest in IMAGE is defined as a forest that has reached its maximum NPP. Hence, this is not the same as a so called 'mature' forest. It takes much longer to get into the mature stage than into the full grown stage.

South America (Appendix A2) shows a large NPP as a result of the tropical woodlands and forests. The South American NPP increases from +0.3 Pg C/yr in 1970 (a source) to -0.8 Pg C/yr in 2100.

The next step was to determine the cause of the large NPP in the tropical and boreal regions (more detailed figures in Appendix B).

Therefore, table 3.2 shows the contribution of full grown forest, regrowing forest and deforestation to the net carbon flux in the year 2100. For boreal forests, the major part comes from the full grown forest for both scenarios (88%). For the tropics, the major part is caused by the regrowing forests (between 50 and 80%), but also the full grown tropical forests (30 to 50%) significantly contribute to the tropical carbon sink.

Table 3.2 Net Carbon fluxes (or Net Ecosystem Productivity (NEP): positive=sink) in the year 2100, divided into full grown vegetation, regrowing vegetation and deforestation (Pg C / yr)

LCT / Fluxes	A1f				B2			
	Full grown vegetation	Regrowing vegetation	Deforestation	Net Flux	Full grown vegetation	Regrowing vegetation	Deforestation	Net Flux
Boreal forest	1.88	0.28	-0.03	2.13	1.27	0.19	-0.01	1.45
Tropical woodland	0.59	1.04	-0.11	1.52	0.29	0.27	-0.04	0.52
Tropical forest	0.49	1.06	-0.06	1.49	0.26	0.56	-0.03	0.79

Expert review

The results were sent to some international experts. They indicated that the cause of the large net sink might be found in:

- Underestimated deforestation areas
- No natural disturbances included in IMAGE2.2
- Overestimated CO₂ fertilisation
- Growth Factor for temperature and soil water availability
- Underestimated recovery periods

Concerning the first bullet, there is an ongoing discussion on global and regional deforestation areas. However, improvements in those parts of the model are already planned in various ongoing research activities, requiring more time, and are thus not pursued further.

Natural disturbances are not explicitly included in IMAGE. Implicitly they have been included in defining the long term 'equilibrium NPP value' of each land cover type. Changes in the frequency of disturbances are not covered by this method.

The last two bullets are part of the carbon cycle within IMAGE, and therefore changeable in the short term and explored in detail in the subsequent sections.

3.4 CO₂ Fertilisation

In IMAGE, CO₂ fertilisation increases the Net Primary Production (NPP). CO₂ fertilisation is calculated as follows:

$$CO_2fert(t)_{m,i} = CO_2fert(1970) * \left(1 + CF_{m,i}(t) * \ln \left(\frac{[CO_2](t)}{[CO_2](1970)} \right) \right)$$

where the CF is a fertilisation factor determined per month (m) and per grid-cell (i). This factor (often called beta factor in literature) depends on a correction function for temperature and soil water status and a correction factor for species characteristics, nutrient availability and altitude (Leemans et al, 2002). In IMAGE 2.2, CF has been limited to a maximum of 0.7.

The beta factor is not constrained by experimental data: its value varies widely from one experiment to another (Körner et al, 2005). Statistical analysis of available data shows that average value of the beta factor measured in controlled exposure studies falls in the range between 0.35 and 0.6 (Alexandrov et al, 2003). Global carbon cycle modellers use a wider range for the annual average beta factor: from 0.2 (Oeschger et al, 1975) to 0.6 (Gifford, 1980). Harvey

(2000) also gives this range between 0.2 and 0.6. IMAGE uses a beta factor (0.43 in average, Appendix C) which is in the range found in literature.

Currently, there's an ongoing discussion on the (quantitative) importance of CO₂ fertilisation. Future climate warming is expected to enhance plant growth in temperate ecosystems and thus increase carbon sequestration. Using free air CO₂ release in combination with a canopy crane, Körner found an immediate and sustained enhancement of carbon flux through 35-meter-tall temperate forest trees when exposed to elevated CO₂. However, there was no overall stimulation in stem growth and leaf litter production after 4 years. Photosynthetic capacity was not reduced, leaf chemistry changes were minor, and tree species differed in their responses. Although growing vigorously, these trees did not accrete more biomass carbon in stems in response to elevated CO₂, thus challenging projections of growth responses, derived from previous tests with smaller trees (Körner et al, 2005). Given a rising atmospheric CO₂ concentration, it is predicted (Cao and Woodward, 1998) that global NEP increases significantly, but that this response will decline as the CO₂ fertilisation effect becomes saturated and is diminished by changes in climatic factors. Four out of six models (Cramer et al, 2001) show a further, climate-induced decline in NEP resulting from increased heterotrophic respiration and declining tropical NPP after 2050. In contrast, another study (Berthelot et al, 2002) assumes that fertilisation will continue to rise until the year 2100. The ongoing discussion on the rising atmospheric CO₂ concentration and the relation to the amount of forest growth increase is still continuing and not expected to be cleared shortly.

In short, since the IMAGE beta value amounts 0.6 in the year 2100, and some experts (including those from the IPCC writing team) point out that the beta factor might well be in between the values 0.2 and 0.3 (or even lower), they considered a value of 0.43 as too optimistic. Furthermore, considering the results of the analysis on scenario A1b, CO₂ fertilisation seems to be responsible for a large part of the high NEP in the year 2100. Therefore, there is a need to explore the consequences of a lower beta factor in IMAGE, and as a consequence lower fertilisation levels.

3.5 Growth factor

The NPP in IMAGE2.2 depends also on a growth multiplier for temperature and soil water availability:

$$GrowthMultiplier(t, l, j) = \frac{(f_1(t, l) * f_2(t, l))}{AF}$$

where:

t the year, l the land cover type and j the grid cell

f₁ (t,l) is a multiplier for direct temperature effect on plant growth

f₂ (t,l) is a multiplier for water availability effect on plant growth

AF is a normalization factor to 1970 average

(Leemans, 2002)

3.6 Recovery period

As indicated, experts thought that the relatively short recovery periods in IMAGE 2.2 could be one of the causes of the large net carbon sink. The recovery period is defined as the amount of years it takes for a land cover type to reach its equilibrium NPP. Note it is not the time it takes to get into the stage of a “mature forest”. This would be (much) longer.

The IMAGE team made a new run with longer recovery periods, as shown in the table below. We realize these new periods might be too long, but to visualize the importance and influence of the recovery periods, these numbers serve well. The results are shown and commented in the next chapter.

Table 3.3 Recovery periods in the original A1f run and for the new run

	IMAGE 2.2 (yrs)	New run (yrs)
Agricultural land	1	1
Extensive grassland	1	1
Regrowth forest (abandoned)*	--	--
Regrowth forest (timber)*	--	--
Ice	0	0
Tundra	5	30
Wooded tundra	5	70
Boreal forest	20	60
Cool conifer	15	50
Temp. mixed forest	15	40
Temp. decid. Forest	10	40
Warm / mixed forest	10	30
Grassland / steppe	2	2
Hot desert	5	5
Scrubland	5	5
Savannah	5	5
Tropical woodland	10	35
Tropical forest	10	25

* Original land cover type numbers are taken here.

4. Simulation experiments

4.1 Introduction

The IMAGE team has run several new simulation runs, to determine the effect of changing certain parameters. The analysis in the previous chapter showed that the large net carbon sink could be caused by CO₂ fertilisation, the multiplier growth and/or the recovery periods. First an analysis has been made to compare the role of CO₂ fertilisation or the climate multiplier on the global and regional NPP fluxes. Then, the results of the new simulation runs (several fertilisation levels as well as longer recovery periods) will be shown.

4.2 NPP: fertilisation versus climate growth factor

To be able to judge the influence of the natural CO₂ fertilisation and the growth multiplier on the NPP, we refer to figures 4.1 and 4.2. These represent the yearly NPP for scenario A1b, for boreal and tropical forests.

The rising NPP in tropical forests is almost completely triggered by CO₂ fertilisation (Figure 4.1). In figure 4.2, the rising NPP for boreal forest without factors is explained by expanding boreal forest areas in time. However, this does not influence the conclusion that in boreal forests both fertilisation and temperature contribute to the increasing NPP.

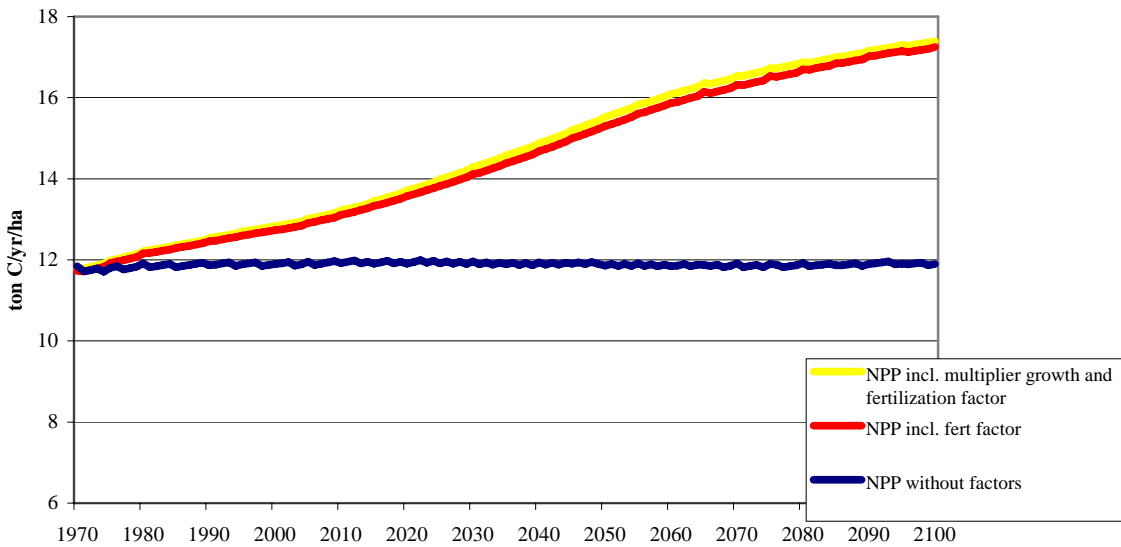


Figure 4.1. NPP in tropical forest for scenario A1b, split into multiplier growth and fertilisation

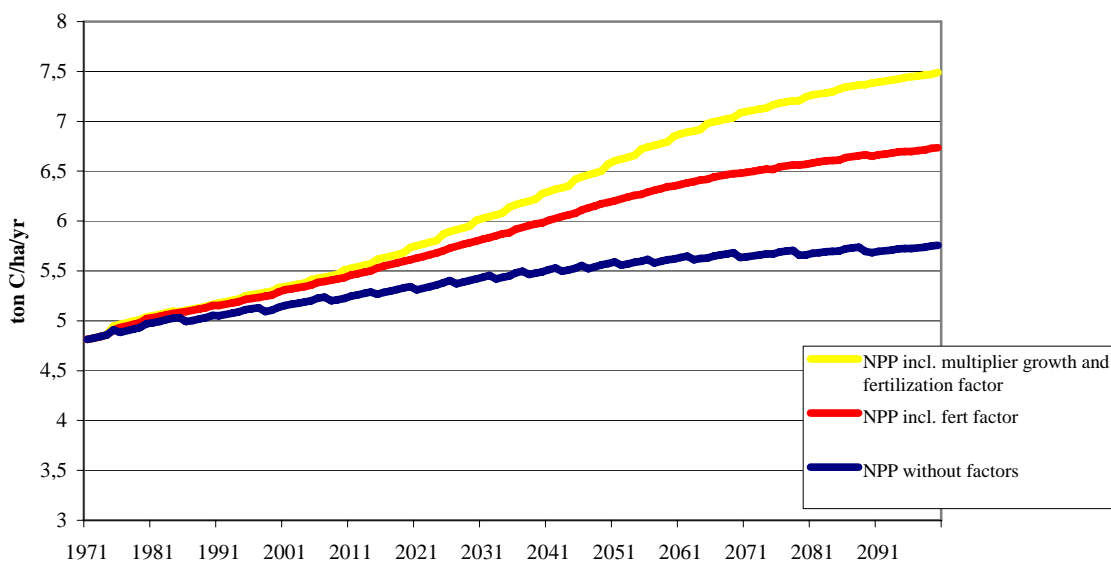


Figure 4.2 NPP in boreal forest for scenario A1b, split into multiplier growth and fertilisation

Figure 4.3 shows that only after 2030 a positive effect takes place in the boreal forests averaged over one full year (+ 10% between 2030 and 2100), which contributes to the large IMAGE sink. The growth multiplier for tropical forests remains constant and worldwide it slightly increases. Again, the world average has been calculated simply by dividing the total sum land cover type Multiplier Growth (MG) by the amount of land cover types. Note that the boreal winter months have a MG of almost zero, while during the summer months the MG is in between 2.4 and 2.6. The boreal year average MG is between 1 and 1.15.

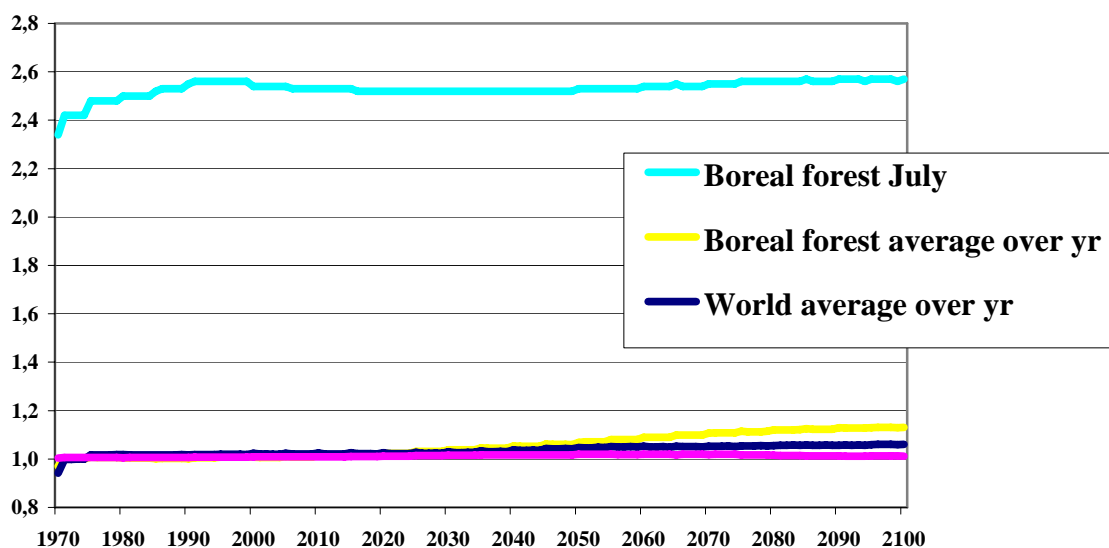


Figure 4.3. The multiplier growth for the original run of A1b, given for boreal and tropical forest, as well as for the world average.

It can be concluded that the main cause of the large net carbon sink is CO₂ fertilisation. The multiplier growth contributes slightly, but not substantially to the boreal net carbon sink.

In chapter 5, new A1f and B2 runs will be made with different fertilisation levels, to analyse the influence of CO₂ fertilisation in more detail on the carbon cycle within IMAGE 2.2.

4.3 CO₂ fertilisation

The IMAGE team made two new runs for both scenarios A1f and B2 showing the impact of 50% fertilisation and of having no natural fertilisation at all. The results show that CO₂-fertilisation has an enormous impact on the carbon cycle and the outcomes of IMAGE.

In contrast to the A1b runs (Appendix C), these runs have been calibrated for the period 1970-2000, and we did not adjust the fertilisation effect on agriculture. That would have caused lower agricultural production rates and therefore a larger demand for agricultural land and consequently more deforestation.

4.3.1 Global scale

The CO₂ fertilisation effect on the global scale is responsible for 16 % of the total NPP in scenario A1f in the year 2100 (Figure 4.4). The increase in NPP since 1970 is caused for 40 % by fertilisation. In scenario B2, fertilisation is responsible for 6 % of the total NPP, while the increase since 1970 is caused for 20 % by fertilisation.

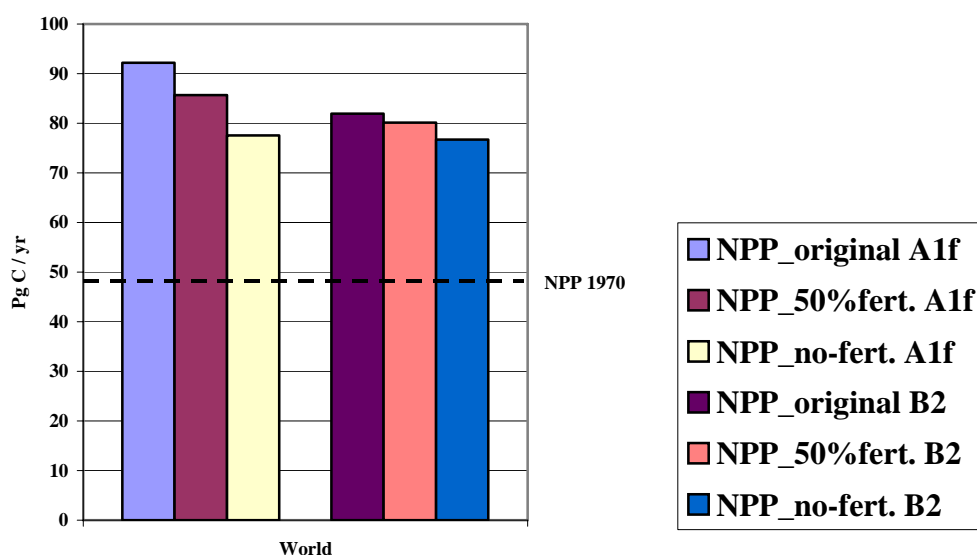


Figure 4.4. The NPP for scenarios A1f and B2, given for the year 2100 and worldwide, showing the consequences of different levels of natural CO₂ fertilisation.

The natural CO₂ fertilisation effect is responsible for 60 % of the total NEP in scenario A1f in the year 2100 (Figure 4.5). The increase in NEP since 1970 is caused for 58 % by CO₂ fertilisation. In scenario B2, fertilisation is responsible for 42 % of the total NEP, while the increase since 1970 is caused for 40 % by fertilisation.

As shown in section 4.2, the growth factor contributes only slightly (less than 10% of the increase worldwide) to the increasing NPP and NEP. The remaining of NPP and NEP is caused by the fertilisation effect on agriculture, since we only adjusted the natural fertilisation effect.

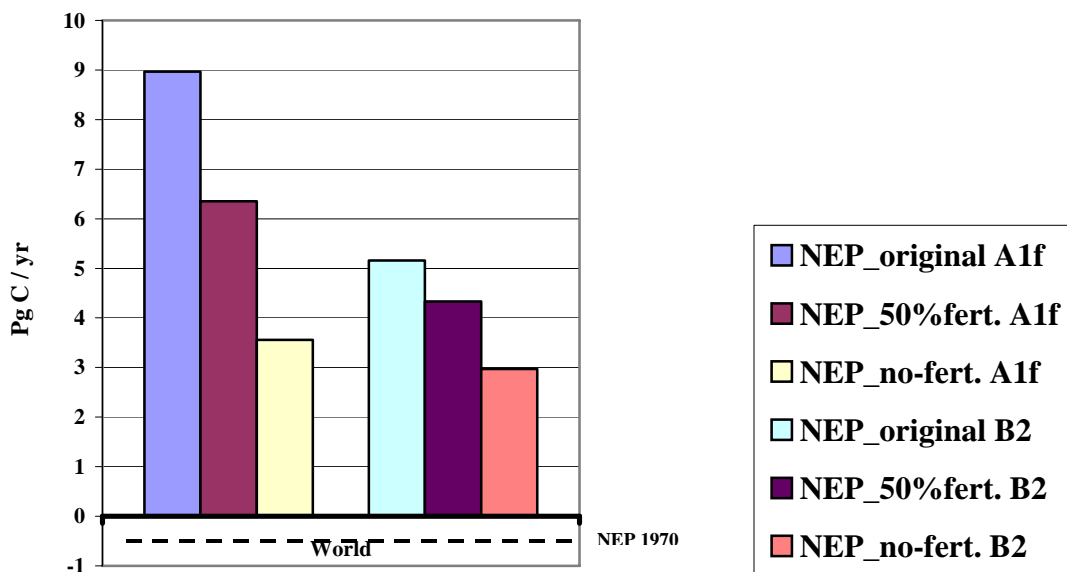


Figure 4.5 The NEP for scenarios A1f and B2, given for the year 2100 and worldwide, showing the consequences of different levels of fertilisation (positive = sink).

4.3.2 Regional carbon dynamics

All regions with large boreal or tropical forest areas do show a sharp decline in NEP when the fertilisation effect is decreased. This ranges from -82% (South America, A1f) to -23% (USA, A1f) (Figure 4.6).

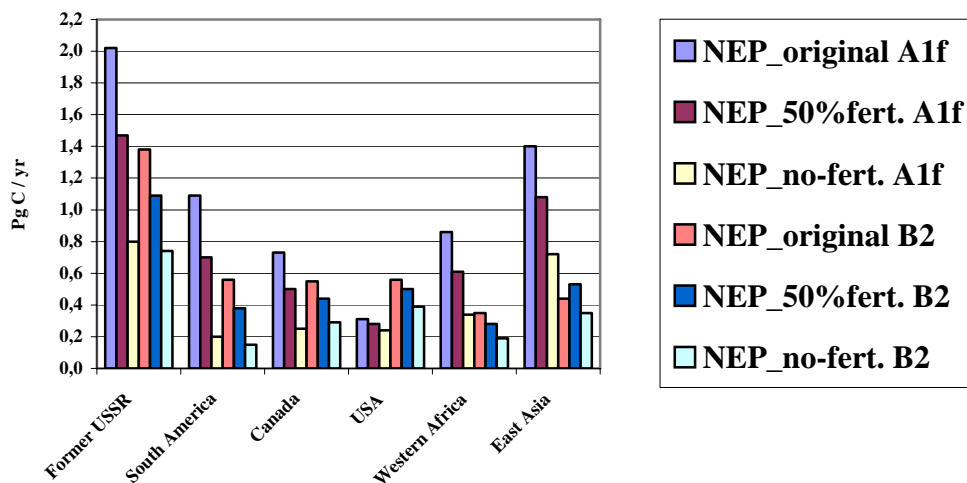


Figure 4.6 The NEP for scenarios A1f and B2, given for the year 2100 and 6 regions, showing the consequences of different levels of fertilisation

Figure 4.7 shows that the 50% fertilisation run has a world average beta factor of about 0.28. As shown before, the 100% fertilisation run gives a beta factor of 0.58 in July. The period 1970-2005 is used for calibration. That's why the beta factor is sharply rising until 2005. Obviously, the no fertilisation run gives a beta factor of zero for the whole period. Figure C2 in Appendix C gives the fertilisation factor per land cover type for scenario A1b, representing the yearly average and the months January and July.

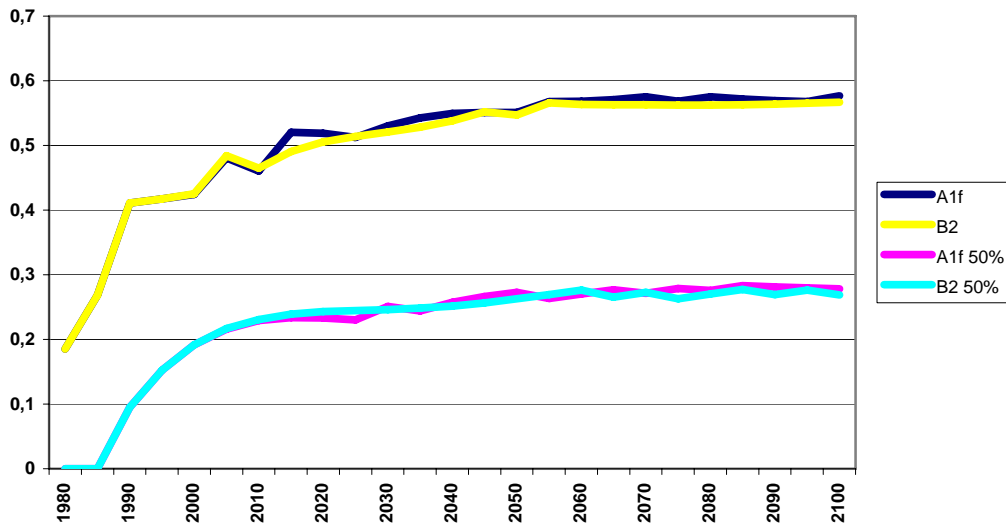


Figure 4.7 World average Beta factor in July for scenarios A1f and B2, for the original runs and the 50% fertilisation runs. The no fertilisation runs gave a beta factor of zero.

The outcome of the new runs of scenarios A1f and B2 have been commented as much more reasonable. The 50% fertilisation runs are within ranges indicated by experts (beta factor between 0.2 and 0.3).

The writer teams of the IPCC WG III chapters 8 and 9 decided to use two baselines per scenario: the 50% and no fertilisation runs. According to them, these baselines cover the uncertainty range of and the discussion on CO₂ fertilisation.

4.4 Grid cell analysis

At the lowest possible level in IMAGE, we followed some grid cells to learn more about the carbon fluxes in the IMAGE model. This has been done for three grid cells in the Former USSR, for which the land cover type remains boreal forest over the whole period and where no deforestation takes place (Figure 4.8 and 4.9).

The different levels of NPP for the different grid cells can be explained by a different location. The grid cell with the highest NPP (red) is located more west in Siberia than the blue, and the blue is again more west than the yellow grid cell. They are all on the same latitude. Both scenarios start at the same NPP level in the year 2000, and split later on (the upper line A1f 50% fertilisation, the lower line A1f No fertilisation).

The three grid cells show an increase over time in NPP as well as in NEP.

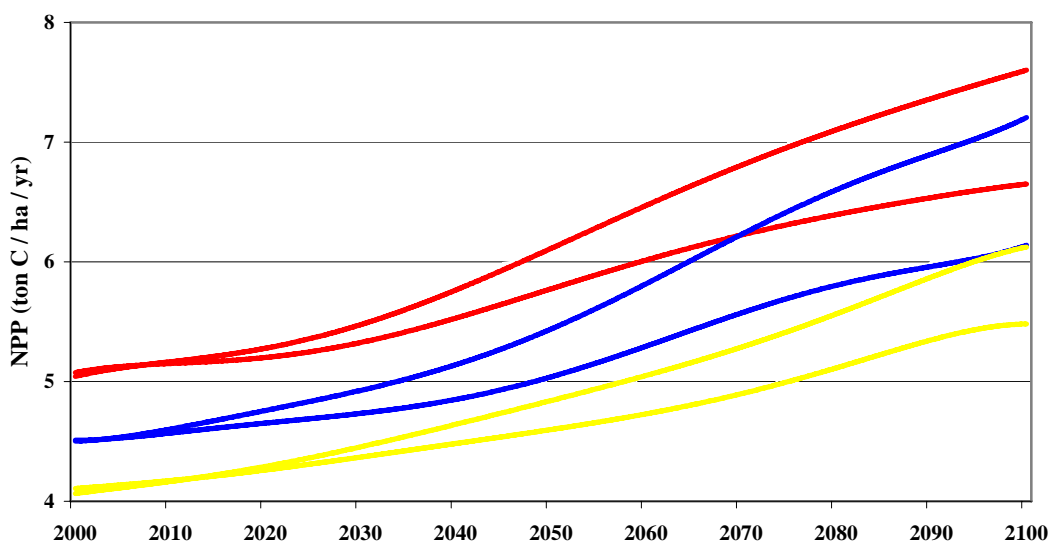


Figure 4.8 Three grid cells (indicated in red, blue and yellow) in the Former USSR, NPP for A1f 50% fertilisation (upper line) and No Fertilisation (lower line) .

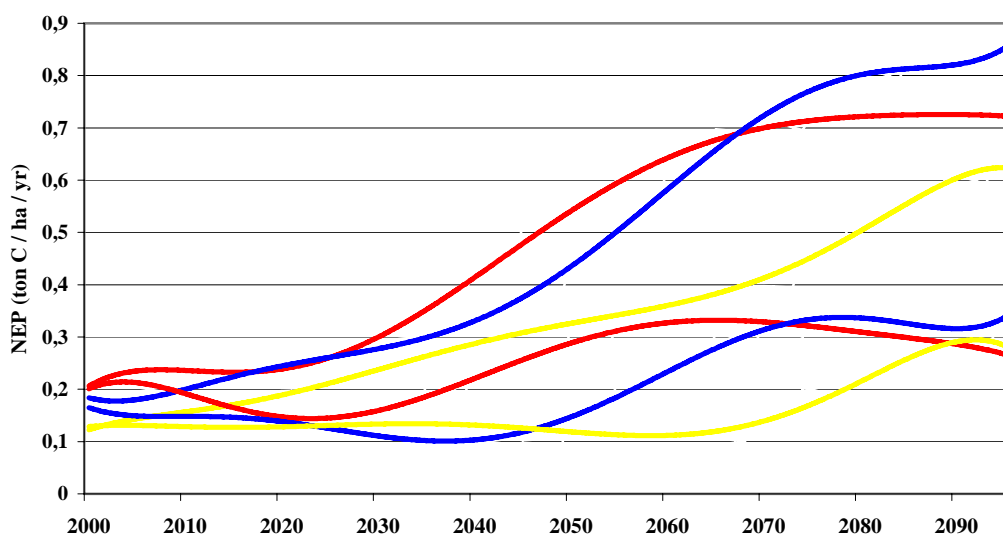


Figure 4.9 Same three grid cells in the Former USSR, but now the NEP for A1f 50% fertilisation and No Fertilisation.

4.5 Recovery period

As explained in section 3.6, a new run has been made with longer recovery periods. Worldwide, the longer recovery periods create a lower NPP (Figure 4.10) and a lower Soil Respiration Flux (Figure 4.11) after the year 2050. The tropical and boreal forests do not or slightly contribute to this increase.

The NPP changes in the original run from 57.4 Gt C / yr in 1970 to 84.8 in 2100. For the longer recovery periods run, the global NPP increases to 83.6 Gt C / yr (minus 1.4% in 2100). The SRF ranges from 56.5 to 79.0 Gt C / yr. For the longer recovery periods run, the global SRF increases up to 78.1 Gt C / yr (minus 1.1% in 2100).

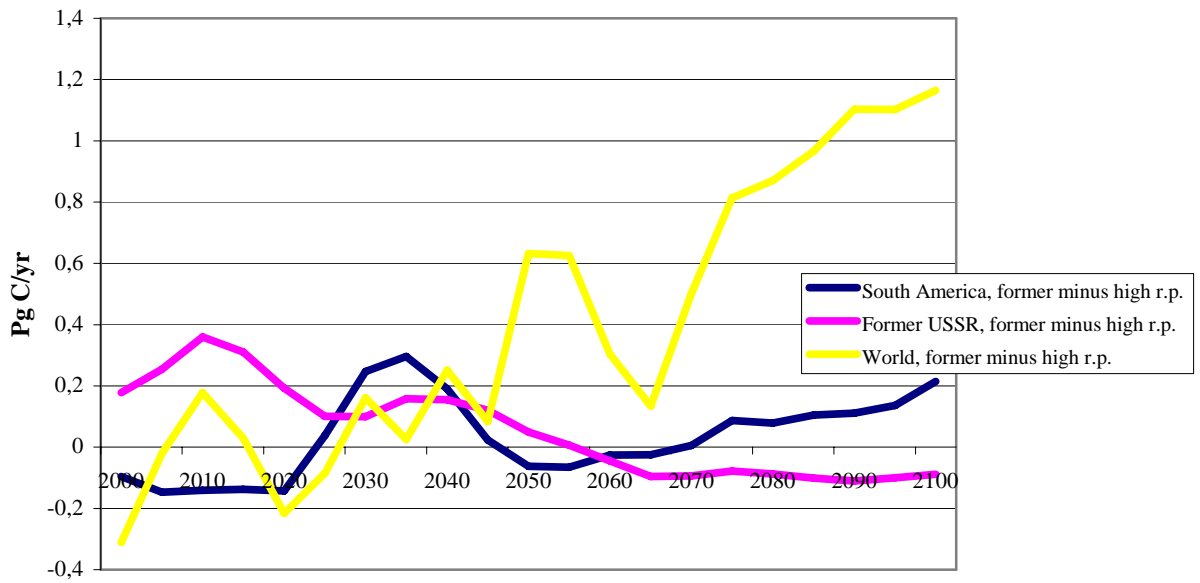


Figure 4.10 NPP for scenario A1b: difference between original run and new run (original run minus new run)

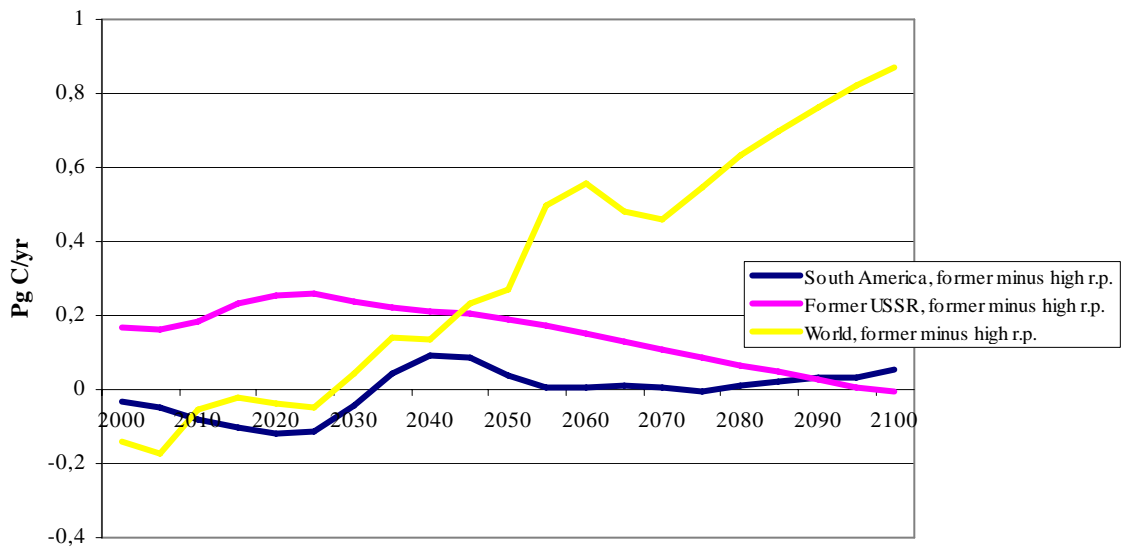


Figure 4.11 SRF for scenario A1b: difference between original run and new run (original run minus new run)

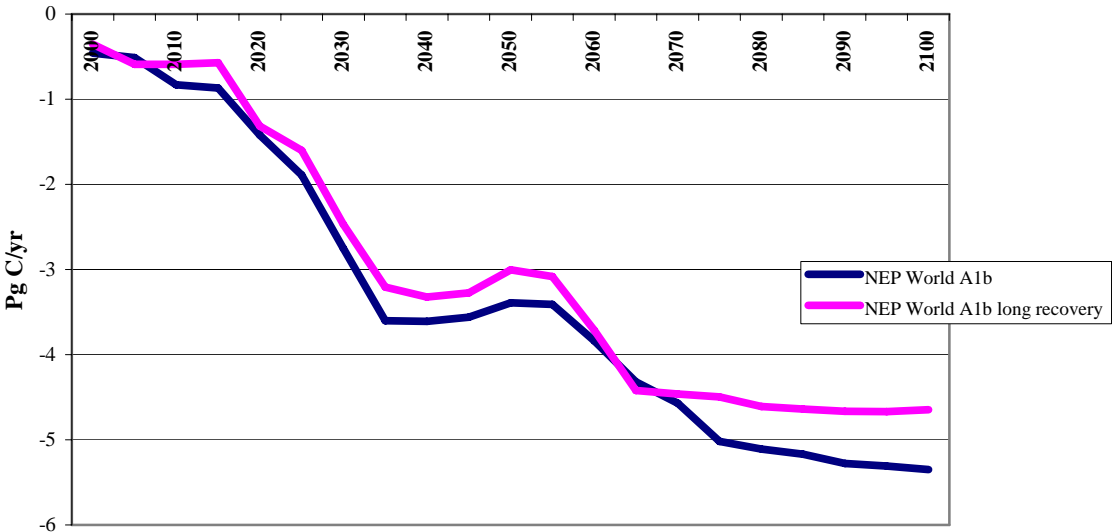


Figure 4.12 NEP for scenario A1b: both the original run and new run

The long recovery run results in a lower net carbon uptake (NEP), with a maximum difference of 0.7 Gton C/yr in 2100 (Figure 4.12). The major part of this originates from the tropical regions. Considering the recovery periods of table 3.3 as maximum values, the large net carbon sink in IMAGE 2.2 could be caused by underestimated recovery periods for a maximum amount of 0.7 Gton C/yr in 2100.

Longer recovery periods have not been implemented into the new baselines, because no sufficient and recent literature could be found to determine better values for the recovery periods. This might be done at a later stage.

5. New Baselines

As discussed in the previous chapter, four new baselines have been constructed: 50% fertilisation of the original run, and no fertilisation at all for scenarios A1f and B2.

5.1 Global scale

Table 5.1 shows that for scenario A1f the net carbon sink in IMAGE has been decreased from 7.33 Pg C/yr (original run) to a source of 0.72 Pg C/yr in the year 2100. Scenario B2 still gives a sink in IMAGE for the year 2100 but it has decreased from 4.01 to 0.89 Pg C/yr.

Table 5.1 yearly net carbon sink (positive) for original IMAGE runs and for new baselines (sum of NEP and deforestation, NBP (Pg C / yr))

Scenario / year (Pg C / yr)	2000	2030	2050	2100
A1f original	0.32	3.26	4.97	7.33
A1f 50% fertilisation	-0.92	1.18	1.21	1.88
A1f No fertilisation	-1.14	-0.13	-0.41	-0.72
B2 original	0.45	2.35	3.58	4.01
B2 50% fertilisation	-0.71	-0.37	1.48	2.25
B2 No fertilisation	-0.96	-1.31	0.22	0.89

Figure 5.1a shows the global NEP and deforestation fluxes separately for the new baselines. It appears that there are almost no differences between the deforestation fluxes for the 50% fertilisation and no fertilisation baselines, since we did not adjust the fertilisation effect on agriculture. That would have caused lower agricultural production rates and therefore a larger demand for agricultural land and consequently more deforestation.

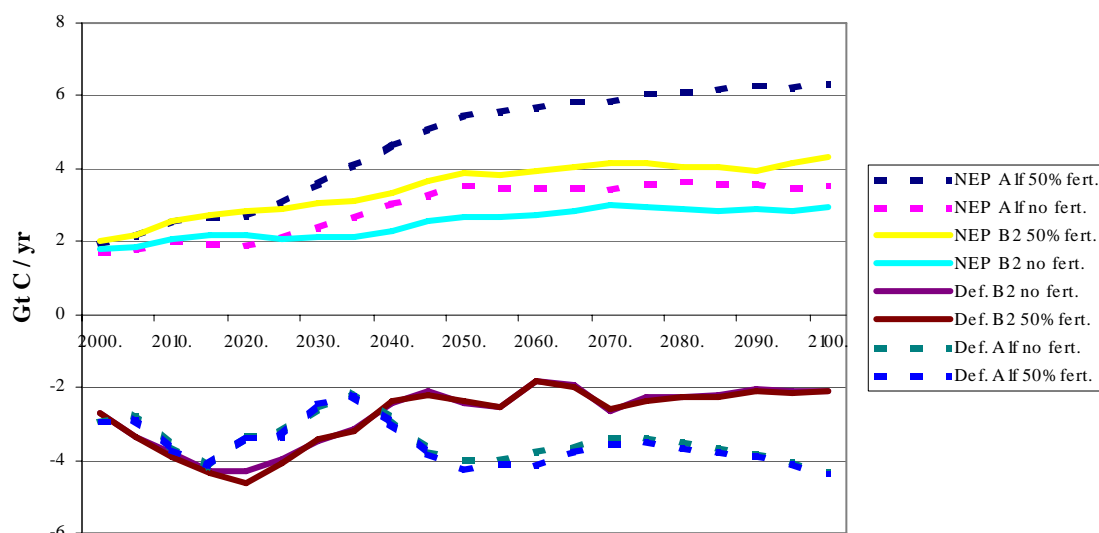


Figure 5.1a Global NEP and deforestation fluxes, for the runs including 50% fertilisation and no fertilisation, scenarios A1f and B2

Figure 5.1b shows the consequences of the changes in fertilisation for the global CO₂ concentration.

The figure shows a large difference between the different runs. The difference between the original run and no fertilisation at all for scenario A1f in the year 2100 amounts 224 ppm, and for B2 133 ppm. For the year 2050 this difference is 81 ppm and 67 ppm respectively.

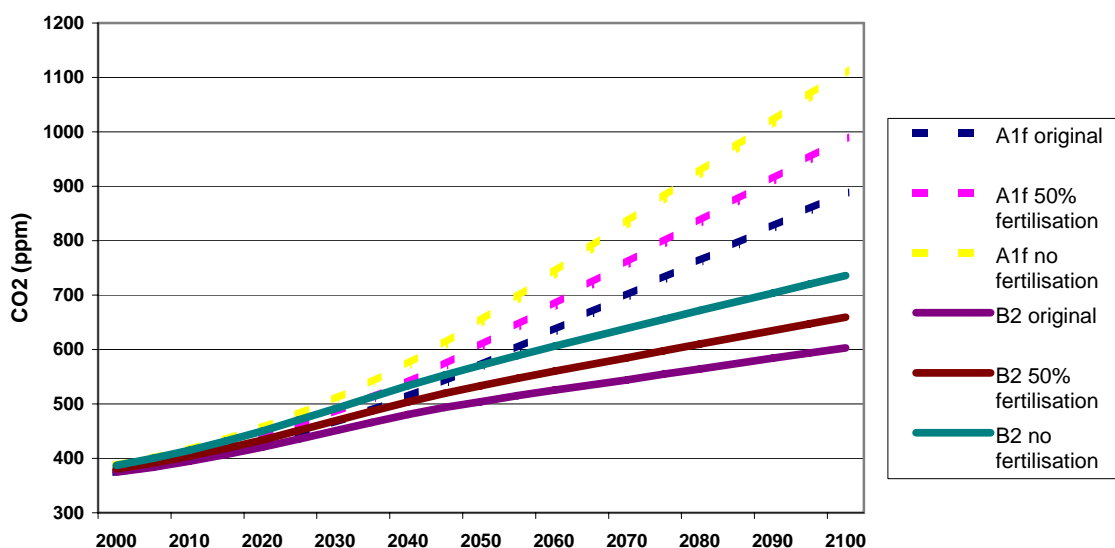


Figure 5.1b Global CO2 concentration, given for scenarios A1f and B2, including the original run, the 50% fertilisation run and the no fertilisation run.

5.2 Regional carbon dynamics

Many regional differences can be found for the net carbon sink. The three main regions we concentrated at are shown below in figures 5.2 to 5.4. Note the different scales per figure. It appears that the Former USSR contributes about 0.3 Pg C/yr (A1f No fertilisation) to 1.0 Pg C/yr (A1f 50% fertilisation and B2 50% fertilisation) to the global sink in the year 2100. Canada contributes between 0.05 Pg C/yr (A1f No fertilisation) to 0.35 Pg C/yr (B2 50% fertilisation) to the global sink, while South America has changed into a source for the year 2100.

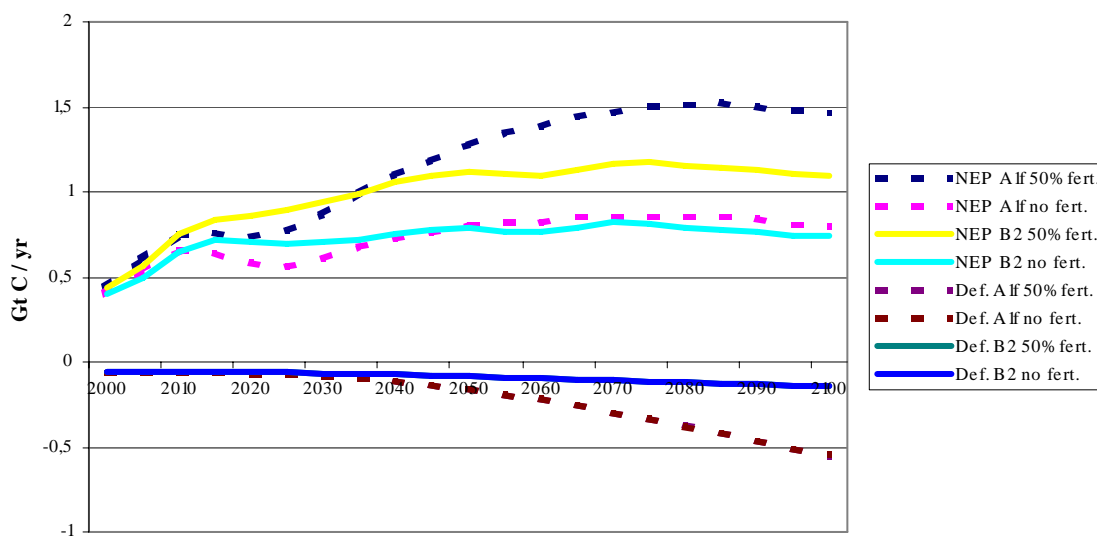


Figure 5.2 The Net Ecosystem Production and the deforestation fluxes in the Former USSR for the runs including 50% fertilisation and no fertilisation, scenarios A1f and B2

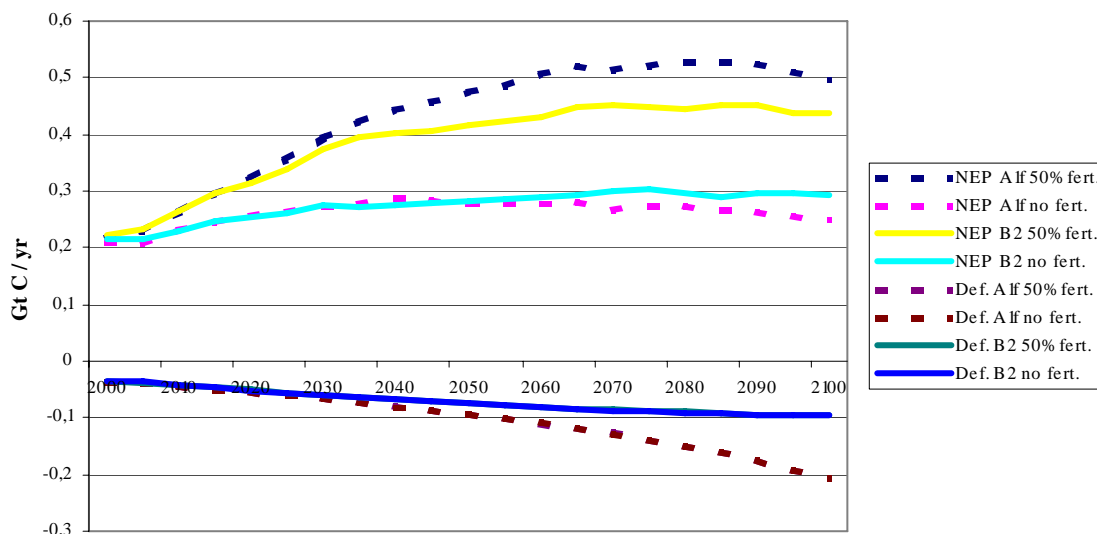


Figure 5.3 The Net Ecosystem Production and the deforestation fluxes in Canada for the runs including 50% fertilisation and no fertilisation, scenarios A1f and B2

Figure 5.4 needs some more attention. Between the years 2020 and 2045 South America is a clear sink for all scenarios.

Scenario A1f gives a sharp increase in deforestation fluxes from the year 2040, which results in a large source from the year 2045, with a peak in 2055 of more than 1 Pg C/yr. From then, the deforestation fluxes decrease again, while the net carbon source decreases to 0.4 (A1f low) or even a sink again (A1f high) for the year 2100. This sharp increase in deforestation (2040-2060) in South America for scenario A1f is caused by the strong economic developments which are incorporated in the A1 scenarios. These economic developments cause a larger food demand and therefore more demand for agricultural land. This agricultural land is being created by deforestation, obviously especially between 2040 and 2060.

Scenario B2 gives a small sink until the year 2070, and then it changes into a small (0.1 to 0.3 Pg C/yr) source.

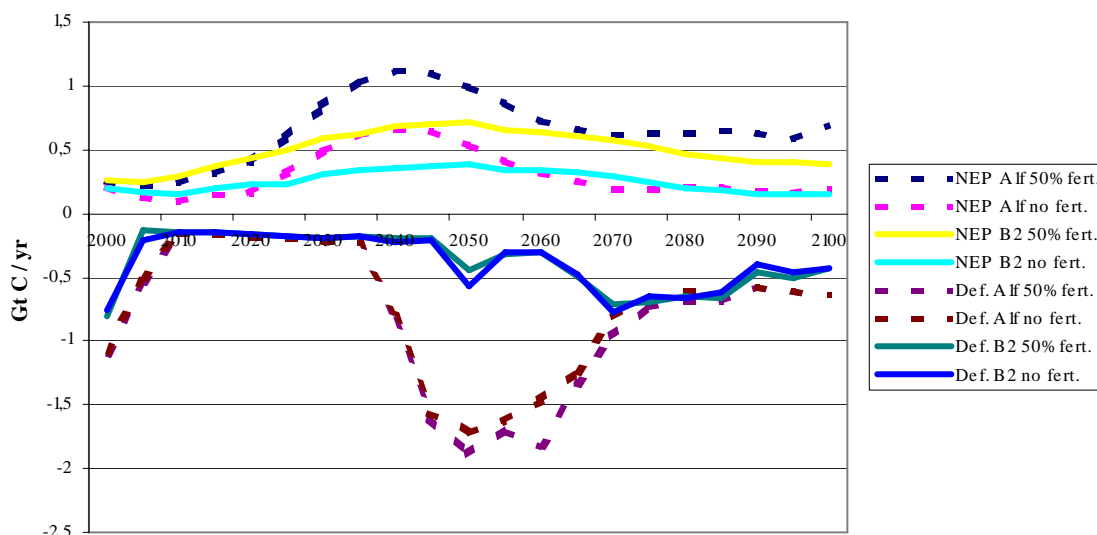


Figure 5.4 The Net Ecosystem Production and the deforestation fluxes in South America for the runs including 50% fertilisation and no fertilisation, scenarios A1f and B2

6. Conclusions

Given the original concerns about the carbon cycle in IMAGE 2.2 and the changes made with respect to the CO₂ fertilisation effect, an important step has been made. However, during the analysis, some other questions and concerns appeared which have to be answered and possibly solved in the (near) future.

It is important to realize that the large net carbon sink in the original baselines (A1f and B2) is probably not only caused by the carbon cycle, but also by other factors, such as assumptions for timber trade, deforestation and natural disturbances. This analysis concentrated on the parameters which were potentially easy to change.

- This analysis made clear that in the original runs the **CO₂ fertilisation** has a major impact on the IMAGE net carbon sink, both on the global and regional scale. As well as for SRES scenario A1f as for B2, the natural CO₂ fertilisation contributes for 60% (A1f) and 42% (B2) to the Net Ecosystem Production (NEP) in the year 2100. The remaining part of the NEP is mainly caused by agricultural CO₂ fertilisation NEP in IMAGE. However, excluding the CO₂ fertilisation effect would give much higher CO₂ concentrations. Reducing the uncertainty for CO₂ fertilisation would also reduce the uncertainty for the baseline runs.
- Since literature on the CO₂ fertilisation effect on natural ecosystems by rising atmospheric CO₂ concentrations is ambiguous, it is difficult to determine what level of CO₂ fertilisation is appropriate. Therefore we defined 2 new baselines (i.e. 50% fertilisation and no fertilisation for natural ecosystems), showing a range for the NPP and NEP that is considered to be more appropriate. **Therefore, 4 new baselines have been constructed:** A1f 50% fertilisation and no fertilisation, and B2 50% fertilisation and no fertilisation. More literature research is needed to get a full overview of recent literature on CO₂ fertilisation, to be better able to reduce the ranges of the CO₂ fertilisation effect in the IMAGE model.
- The land cover types that caused the large net carbon sink are boreal and tropical forests. For boreal forests the sink was only found in the full grown forests. For tropical forests both **full grown and regrowing forests** contributed to the sink.
- Increasing the recovery periods only had a relatively small effect on the net carbon sink. The assumed (too) short **recovery periods** contribute for a maximum of 0.7 Gton / yr. Nevertheless, it might be worth to change these data using more recent insights on recovery periods, if available.
- There is discussion on the IMAGE **deforestation** areas, as well as on worldwide deforestation areas in general. The IMAGE team should follow this discussion closely and act if necessary. Recent trends are not (yet) implemented in IMAGE 2.2, but are of significant influence on the land use carbon sink.

Acknowledgement

After more than two months of hard work and good cooperation, I hope these results will contribute to better understanding of the carbon cycle within IMAGE, and the carbon cycle in general. For further negotiations about the post Kyoto period, it is necessary to better understand and project the net LULUCF carbon sink. I sincerely hope the IMAGE model can contribute to this discussion, including the results of this analysis.

I would like to thank some people who made this analysis to what it is now. First of all the IMAGE team, namely Jelle van Minnen, Bart Strengers en Detlef van Vuuren. They solved many problems and made new (baseline) runs when necessary. Secondly, Gert Jan Nabuurs, who represented the IPCC WG III chapters 8 and 9. He kept us on the right track to finally be able to produce useful baseline runs. Many thanks to the other chapter 8 and 9 authors as well. Without their comments this analysis would have been less useful. Thirdly, thanks to Eveline Trines, who helped me starting this project and improving this report. Finally, I would like to thank the Dutch Ministry of Agriculture, Nature Management and Food Quality (LNV), financing this project.

Literature

- Alcamo, J., R. Leemans and E. Kreileman (eds), *Global change scenarios of the 21st century. Results from the IMAGE 2.1 model*. Pergamon & Elseviers Science, London. pp 296, 1998
- Alexandrov, GA, Oikawa, T, Yamagata, Y, *Climate dependence of the CO₂ fertilisation effect on terrestrial net primary production*, Tellus, Vol. 55b, 669-675, 2003
- Berthelot, M, Dufresne, JL et al, *Global response of the terrestrial biosphere to CO₂ and climate change using a coupled climate-carbon cycle model*, Global Biogeochemical Cycles, Vol. 16, No. 4, 1084, 2002
- Cao, M and Woodward, I, *Dynamic responses of terrestrial ecosystem carbon cycling to global climate change*, Nature, 393, 249-252, 1998
- Ciais, Ph. Et al., *Europe-wide reduction in primary productivity caused by the heat and drought in 2003*, Nature, vol. 437, 529-533, 2005
- Cramer, W, Bondeau, A, Woodward I et al, *Global response of terrestrial ecosystem structure and function to CO₂ and climate change: results from six dynamic global vegetation models*, Global Change Biology, 7, 357-373, 2001
- Gifford, RM, *Carbon storage by the biosphere*, Carbon dioxide and climate, Australian Academy of Sciences, Canberra, 167-181, 1980
- Harvey, LD, *Global warming, the hard science*, 160-162, Pearson Education Limited, Essex, 2000
- IPCC, *Special report on emission scenarios*, Cambridge University Press, 2000
- Joos, F., M. Bruno, R. Fink, U. Siegenthaler, T.F. Stocker, C. Le Quéré and J.L. Sarmiento, *An efficient and accurate representation of complex oceanic and biospheric models of anthropogenic carbon uptake*. Tellus, 48B, 397-417, 1996
- Klein Goldewijk, K., J. van Minnen, E. Kreileman, M. Vloedbeld and R. Leemans, *Simulating the carbon flux between the terrestrial environment and the atmosphere*. Water, Air and Soil Pollution, 76, 199-230, 1994
- Körner, C, Asshoff, R, et al, *Carbon flux and growth in mature deciduous forest trees exposed to elevated CO₂*, Science, vol. 309, 1360-1362, 2005
- Leemans, R. et al, *The consequences of uncertainties in land use, climate and vegetation responses on the terrestrial carbon*, Science in China, Vol. 45, 126-141, 2002
- Marland, G., T.A. Boden and R.J. Andes, *Global, regional and national CO₂ emissions*. In: Trends: A Compendium of Data on Global Change. Carbon Dioxide Information Analysis Center, Oak Ridge National Laboratory, U.S. Department of Energy, Oak Ridge, Tenn., USA, 2000
- Oeshger, H, Siegenthaler, U, Schooterer, U, Gugelmann, A, *A box diffusion model to study the carbon dioxide exchange in nature*, Tellus, Vol. 27, 168-192, 1975

Appendix A

Figure A1, Net Carbon Flux (sum of full grown, regrowing and deforestation) for South America

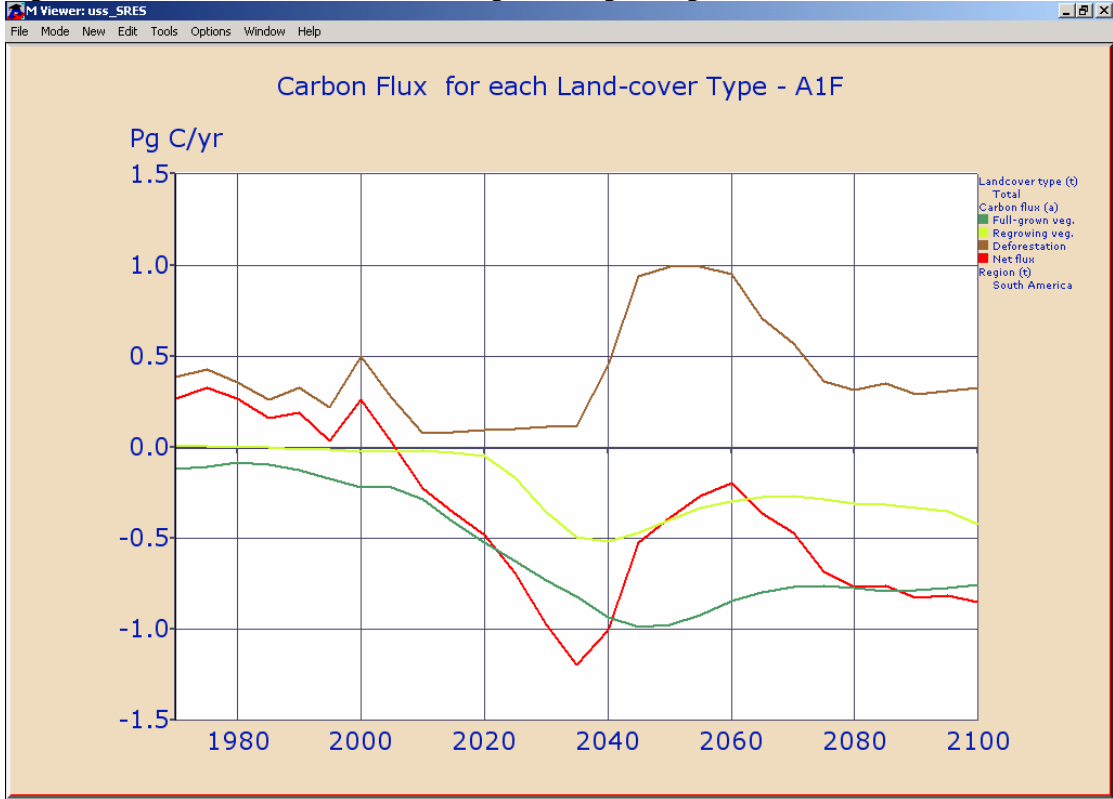
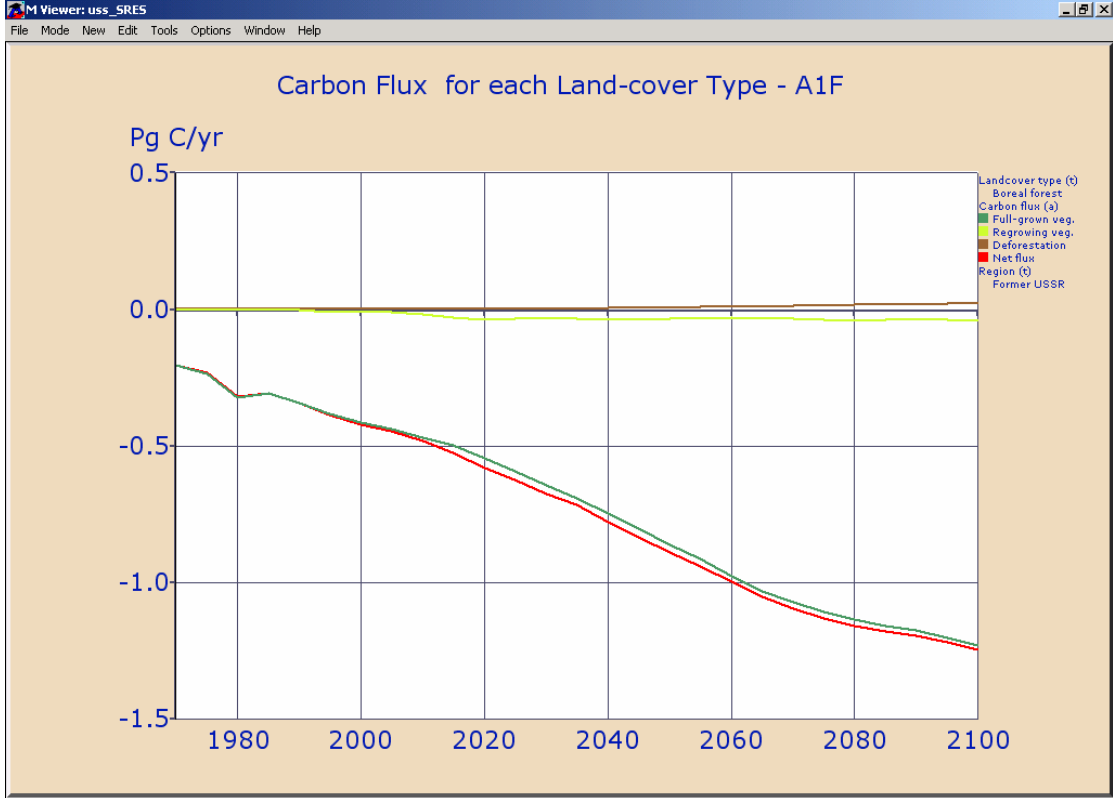


Figure A2, Net Carbon Flux (sum of full grown, regrowing and deforestation) for Former USSR



Appendix B

Figure B1, Net Carbon Flux (sum of full grown, regrowing and deforestation) for all land cover types (negative = sink), NB: agricultural land is a source, since it is created by deforestation

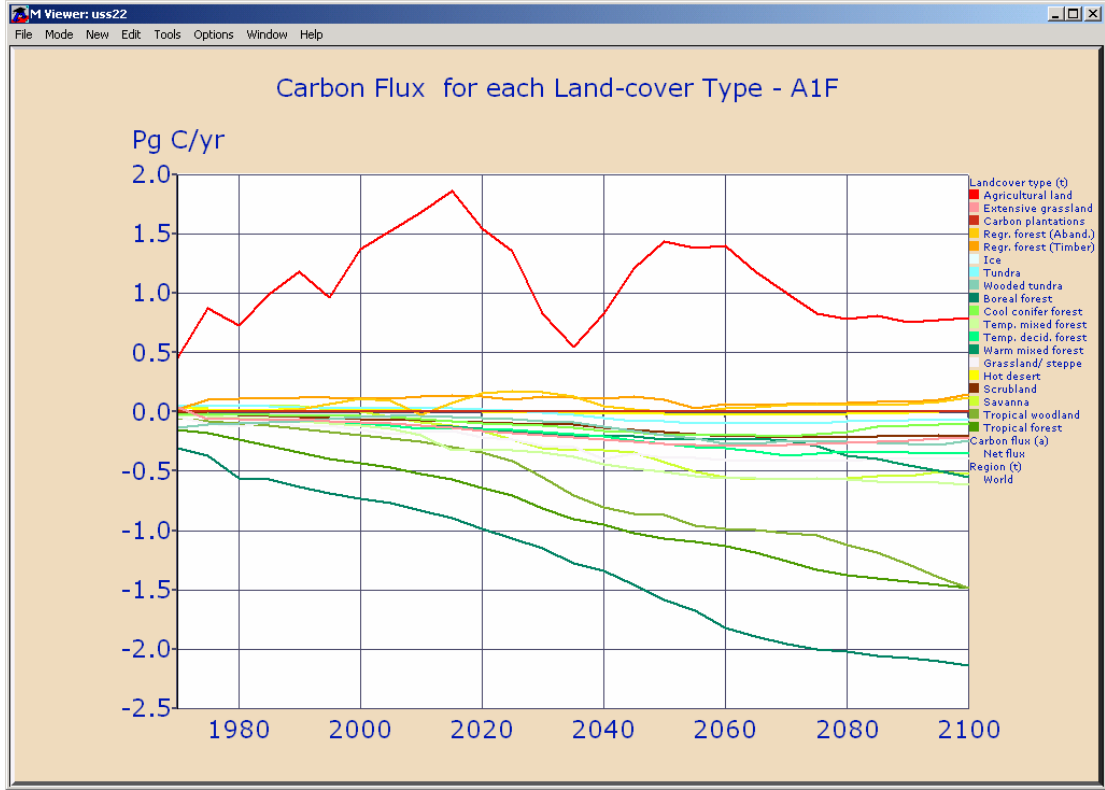


Figure B2, Net Carbon Flux (sum of full grown, regrowing and deforestation) for all regions (negative = sink):

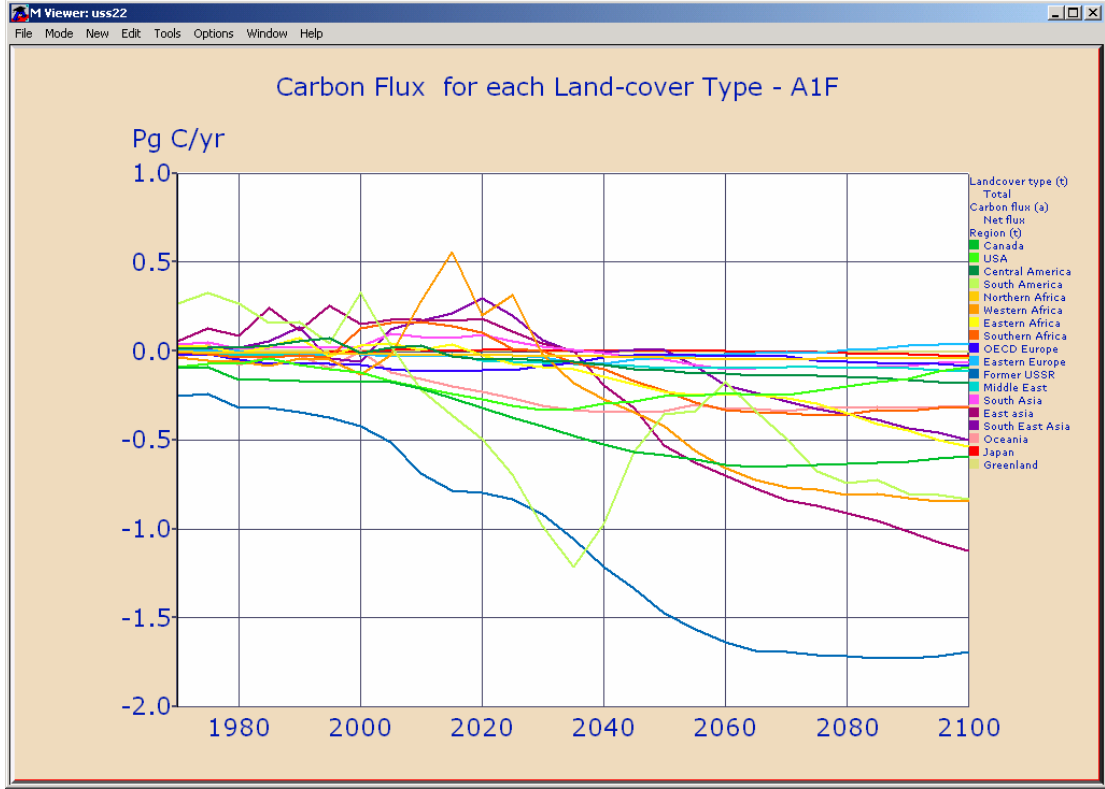


Figure B3, Net Carbon Flux (sum of full grown, regrowing and deforestation) for all land cover types (negative = sink) NB: agricultural land is a source, since it is created by deforestation

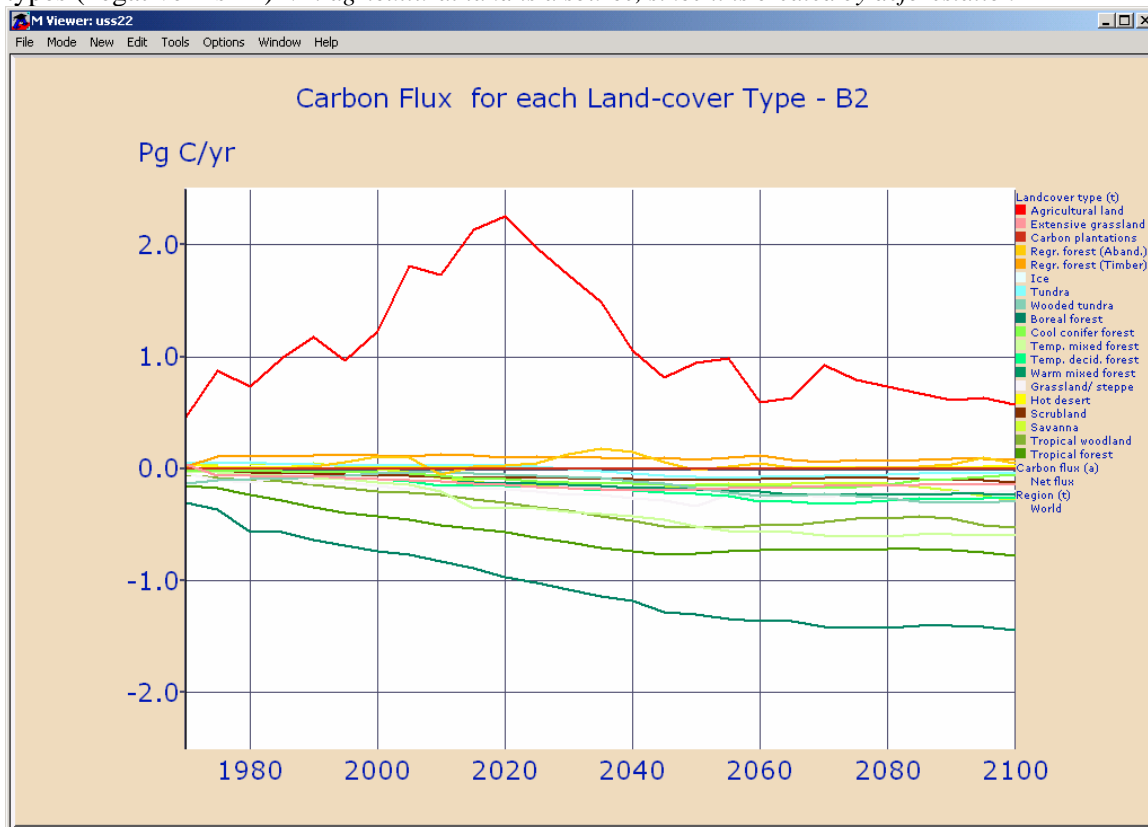
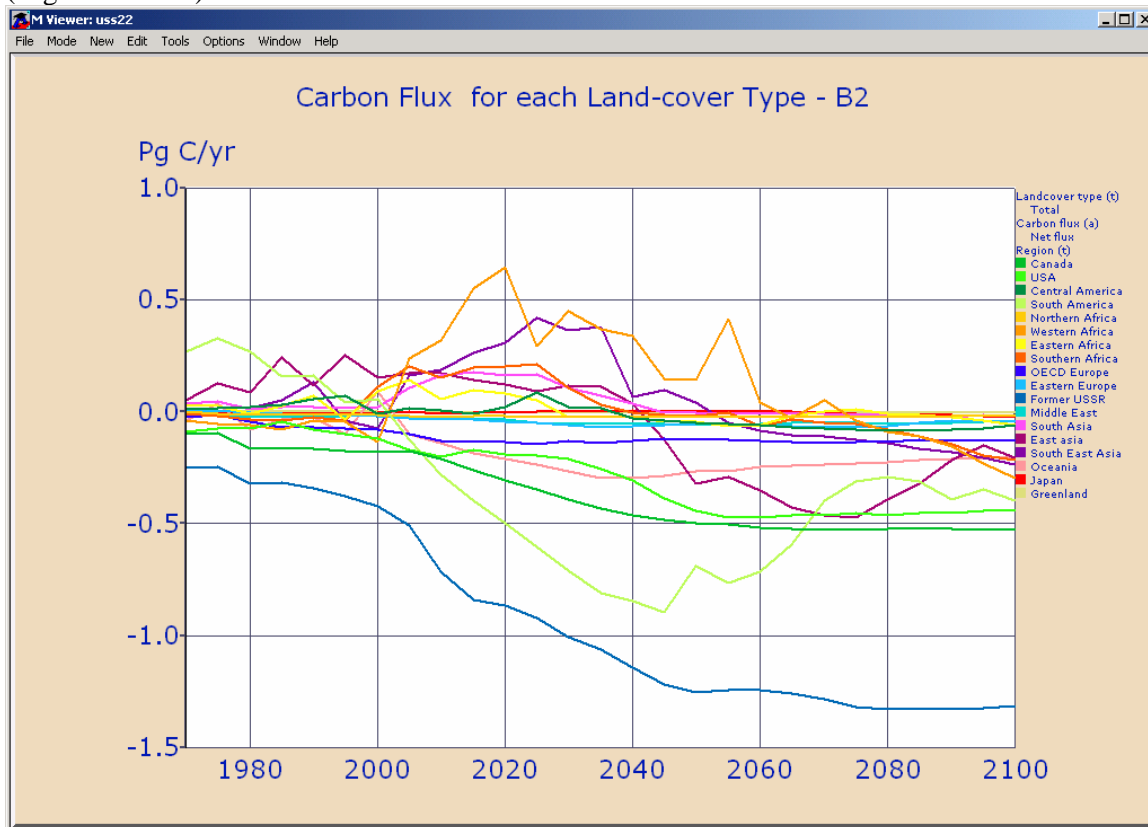


Figure B4, Net Carbon Flux (sum of full grown, regrowing and deforestation) for all regions (negative = sink)



Appendix C

Beta Factor and CO₂ fertilisation for scenario A1b

Table C1. Scenario A1b with and without fertilisation, and uptake due to fertilisation

Regions	Year	NEP A1b (Pg C/ yr)	NEP A1b no fert. (Pg C/ yr)	Uptake due to fertilisation (Pg C/ yr)
Canada	2000	-0.18	-0.17	0.01
	2030	-0.43	-0.21	0.22
	2050	-0.55	-0.19	0.36
	2100	-0.50	-0.07	0.43
USA	2000	-0.12	-0.10	0.02
	2030	-0.29	-0.05	0.24
	2050	-0.23	0.12	0.35
	2100	0.04	0.30	0.26
South America	2000	0.26	0.23	-0.03
	2030	-0.94	-0.23	0.71
	2050	0.05	1.2	1.15
	2100	-0.44	0.41	0.85
Western Africa	2000	-0.12	-0.08	0.04
	2030	0.01	0.34	0.33
	2050	-0.01	0.41	0.42
	2100	-0.67	-0.18	0.49
Former USSR	2000	-0.42	-0.38	0.04
	2030	-0.91	-0.39	0.52
	2050	-1.36	-0.46	0.90
	2100	-1.24	-0.13	1.11
World	2000	-0.44	-0.34	0.10
	2030	-2.7	0.60	3.3
	2050	-3.4	1.8	5.2
	2100	-5.3	-0.10	5.2

The beta factor in IMAGE2.2 in the original run for scenario A1b, is more or less constant at 0.55 for boreal forest during summer (July) and for boreal forest averaged over the whole year it is about 0.20. For tropical forest the beta factor is about 0.53 and more or less constant over all months. The world beta factor (averaged over all land cover types) is about 0.43 (Figure C1).

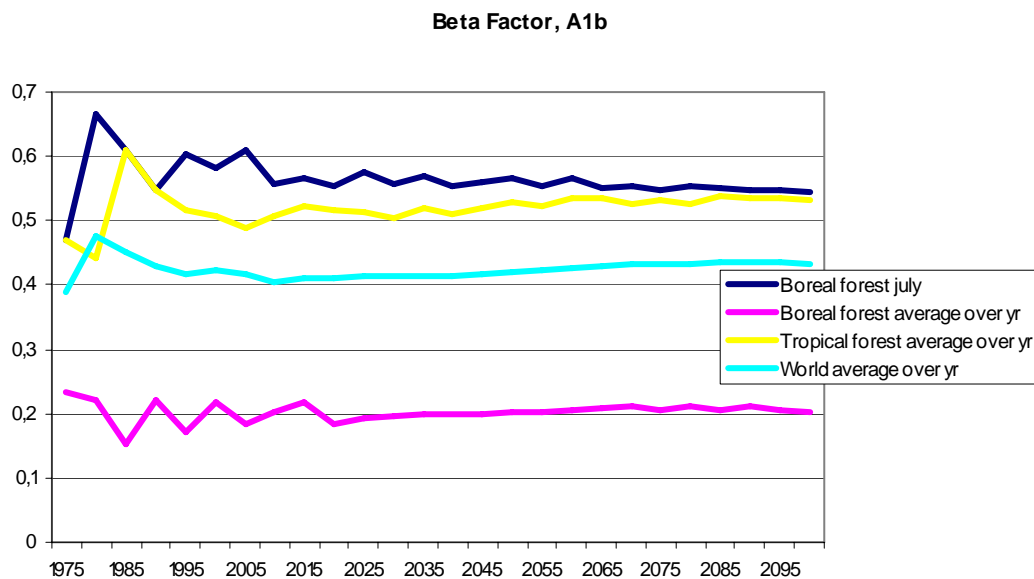


Figure C1 Beta Factor for the original run of scenario A1b, given for boreal and tropical forest, as well as the world average

The fertilisation factor per land cover type for the original A1b run is shown in figure C2 . Here you may see the differences per month (between January and July), as well as the averaged value over the whole year. This is simply (and arbitrarily) done by dividing the sum of all months by twelve.

Please note that there's (almost) no difference between January and July for the tropical region and that the differences are large(r) for the temperate latitudes.

Fertilisation factor per land cover type in 2100

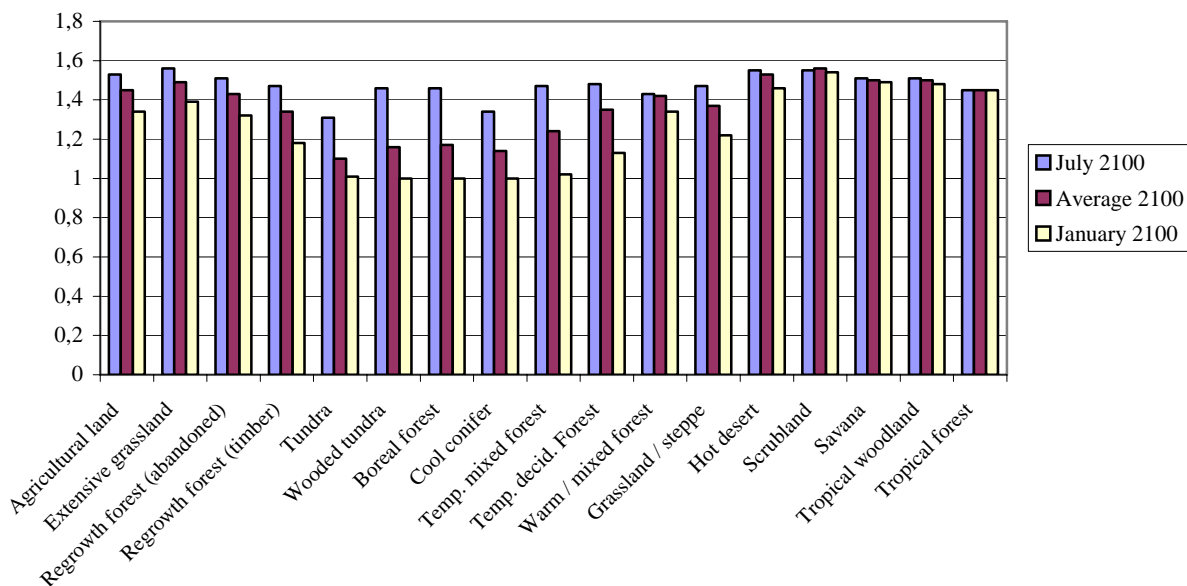
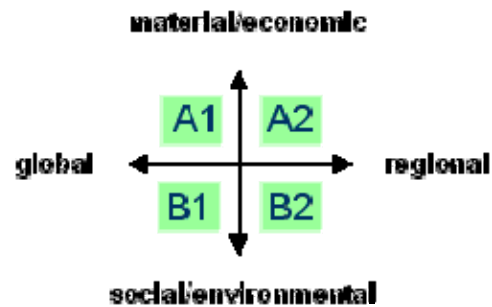


Figure C2. The fertilisation factor ($= 1 + CF_{m,i} * LN ([CO_2](t) / [CO_2] (1970))$) per land cover type in the year 2100, when it is at its maximum, for scenario A1b.

Appendix D

In 2000, the IPCC published a set of new scenarios in the Special Report on Emissions Scenarios (SRES). These scenarios are based on a thorough review of the literature, the development of narrative 'storylines' and the quantification of these storylines using six different integrated models from different countries. These storylines were constructed on two axes, i.e. the degree of globalisation versus regionalisation, and the degree of orientation on material versus social and ecological values. The four clusters were given simple names:



The **A1 storyline** and scenario family describes a future world of very rapid economic growth, low population growth, and the rapid introduction of new and more efficient technologies. Major underlying themes are convergence among regions, capacity building and increased cultural and social interactions, with a substantial reduction in regional differences in per capita income. The A1 scenario family develops into three groups that describe alternative directions of technological change in the energy system. The three A1 groups are distinguished by their technological emphasis: fossil intensive (A1F), non-fossil energy sources (A1T) and balanced across all sources (A1B).

The **B2 storyline** and scenario family describes a world in which the emphasis is on local solutions to economic, social, and environmental sustainability. It is a world with moderate population growth, intermediate levels of economic development, and less rapid and more diverse technological change than in the B1 and A1 storylines. While the scenario is also oriented toward environmental protection and social equity, it focuses on local and regional levels. (IPCC, 2000)